

Kinetics of Autoxidation of Atactic Polypropylene by Infrared Spectroscopy

B. R. JADRNICEK* and S. S. STIVALA, *Department of Chemistry and Chemical Engineering, Stevens Institute of Technology, Hoboken, New Jersey 07030*, and LEO REICH, *Polymer Research Branch, Picatinny Arsenal, Dover, New Jersey 07801*

Synopsis

The autoxidation of a film of atactic polypropylene was studied by means of infrared spectroscopy. Reaction temperatures varied from 110° to 135°C and oxygen concentrations, from 5% to 100% by volume. A general reaction scheme previously reported for the autoxidation of polyolefins was utilized for atactic polypropylene. Various results obtained for this polymer were compared with those previously reported for isotactic polypropylene.

INTRODUCTION

A general kinetic scheme for the uncatalyzed, uninhibited autoxidation of isotactic polypropylene (IPP) in the bulk phase was first reported by Stivala and Reich in 1963.^{1,2} Since then, they have reported on various kinetic aspects of the autoxidation of polyolefins using this general scheme. The thermal oxidation kinetics of films of IPP,²⁻⁶ atactic polybutene-1 (APB),^{6,7} and isotactic polybutene-1 (IPB)⁸ were studied by infrared spectroscopy as a function of temperature and oxygen-nitrogen ratios by observing rates of carbonyl and hydroperoxide formation. Activation energies were estimated for various steps in the scheme. We have found that the scheme and the corresponding mathematical expressions satisfactorily explain the experimental results obtained. Furthermore, results obtained for polypropylene (PP) and polybutene-1 (PB) by other investigators, i.e., rate of formation of volatile products,^{4,6,9,10} chemiluminescence,^{5,11,12} oxygen absorption,^{5,11,12} and changes in intrinsic viscosity as a function of time^{13,14} could also be accounted for by means of the scheme.

Recently, Bawn and Chaudhri^{15,16} successfully applied the general scheme presented by Reich and Stivala to the autoxidation of atactic polypropylene (APP) in solution, at relatively high polymer concentrations. At relatively low polymer concentrations, a much simpler scheme was found to be valid in which the termination of polymeric peroxy radicals by recombination was postulated,¹⁷ which the general scheme mentioned

* Postdoctoral Fellow, 1969-1970.

earlier did not include. Further, work carried out by Bawn and Chaudhri for rate of formation of carbonyl and intrinsic viscosity changes in concentrated APP solutions was expanded by Reich and Stivala,¹⁸ utilizing the general scheme.

The purpose of this paper is to extend the work of Reich and Stivala for the autoxidation of polyolefins to APP in the bulk phase by means of infrared spectroscopy.

EXPERIMENTAL

Starting Material

An uninhibited sample of atactic polybutene-1 (APP), obtained from Avisun Corporation, was refluxed with diethyl ether for 2 hr, and insoluble residue (presumably an isotactic fraction) was removed by filtration through glass wool. The resulting filtrate was slowly added to methanol to precipitate the APP. The precipitate was repeatedly washed with methanol and dried at room temperature under vacuum. The dried APP was redissolved in diethyl ether and reprecipitated and rewashed with methanol. This procedure was repeated once more. The dried APP was finally purified by passing its ether solution through a column of aluminum oxide. The APP was precipitated from the resulting eluent and dried under vacuum at 40°C for 2 hr.

The yield, based on the original weight of APP, was about 60 wt-%. An infrared spectrum of the dried APP was similar to that reported by Luongo.²⁰ From this spectrum it was ascertained, using the bands at 974 and 995 cm^{-1} ,¹⁹ that the sample was close to 100% atactic. Upon ignition, the APP sample gave an ash content of 0.008%, and by the use of a membrane osmometer a number-average molecular weight of 30,000 was obtained.

Apparatus

For the infrared spectra, a Perkin-Elmer recording spectrophotometer, Model 21, was employed. Attached to this instrument was an oxidation cell which was essentially similar to that described previously; it is depicted in Figure 1.² Briefly, the cell consists of a brass cylindrical body into which are introduced a standard salt plate, an aluminum spacer, a salt plate holder, a second salt plate containing the film specimen, and a threaded lock ring. The body of the cell is equipped with a temperature-controlling thermistor, a reaction temperature-indicating thermistor, and numerous turns of heating wire. A $\frac{1}{4}$ -in. metallic orifice perpendicular to the main body of the cell is used to admit gas, e.g., O_2 and $\text{O}_2\text{-N}_2$, and a second smaller opening at the opposite end permits the escape of the gas. The temperature controller, Thermonitor Model ST (E. H. Sargent & Co.) had a temperature range up to 150°C, with a nominal temperature variation of $\pm 0.05^\circ\text{C}$. The cell chamber temperature was measured with

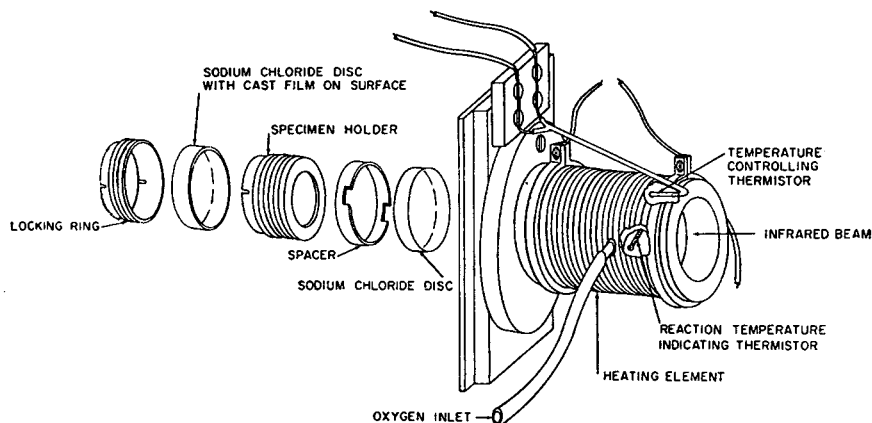


Fig. 1. Oxidation cell.

an iron-Constantan thermocouple connected to a millivolt potentiometer (Leeds & Northrup). The Thermonitor temperature reading was calibrated against the potentiometer.

For the quantitative estimation of carbonyl content in the oxidized APP as ketones and aldehydes, in the form of hydrazones, a Beckman DU spectrophotometer, Model 2400, was used.

Procedure

Purified APP was dissolved in carbon tetrachloride, and a portion of this solution was poured onto an optical sodium chloride disc attached to which was a Teflon gasket serving as a mold. Films of about $2\frac{1}{2}$ -mil thickness were obtained by slow evaporation of the solvent at room temperature and by drying under vacuum for ca. 30 min. The films on the sodium chloride discs were assembled in the oxidation cell (Fig. 1) which was then attached to the infrared spectrophotometer. Known amounts of purified oxygen and nitrogen mixtures (purified by means of sodium hydroxide and anhydrous calcium chloride) were passed into the oxidation cell at a constant rate of 30 ml/min after the desired reaction temperature had been reached. (Prior to reaching this temperature, the APP sample was heated under a blanket of nitrogen.) The ratios (by volume) of oxygen to nitrogen mixtures used were: 5/95, 10/90, 20/80, 50/50, 75/25, and 100/0. Reaction temperatures ranged from 110°C to 130°C. Infrared spectra of the carbonyl region were recorded as a function of reaction time. Apparent weight losses of APP films during oxidation due to volatile product formation were found to be low. Thus, after 4 hr at 130°C and 100% oxygen, the weight loss was less than 1%.

Rate of Carbonyl Formation

The infrared carbonyl absorption band (5.4–6.1 μ) was found to be generally broad and lacking in discreteness (except for the carboxyl group

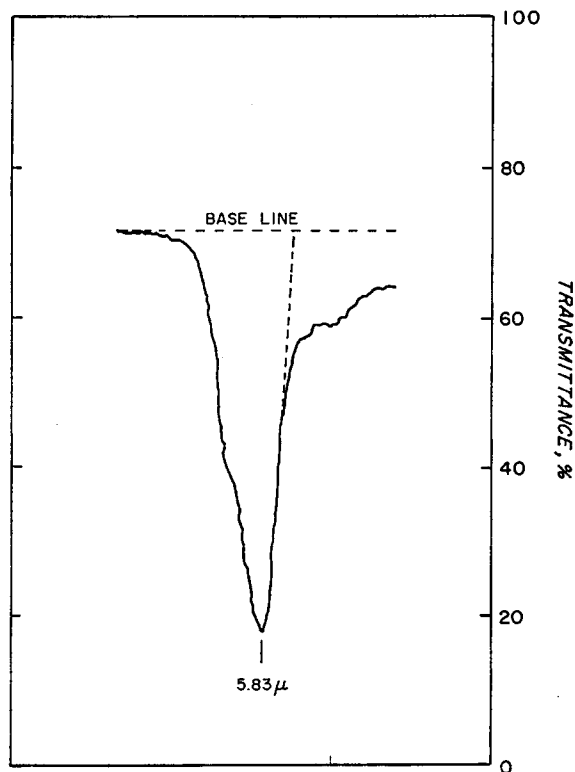


Fig. 2. Area limits used in measuring carbonyl content.

absorption peak at 5.83μ). The amount of carbonyl (from aldehydes, ketones, acids, and esters) formed as a function of time was measured in terms of the total absorbance area (cm^2) of the carbonyl band (the recorded transmittance band, Fig. 2, was replotted in units of absorbance) in order to obtain kinetic data. These absorbance areas were directly proportional to total carbonyl concentration (see next section). The resulting data were then used to verify kinetic expressions derived from the assumed general mechanism.¹

Validity of the Lambert-Beer Law

As mentioned above, carbonyl absorbance areas formed during oxidation of APP were used as a measure of total carbonyl concentration to obtain kinetic data. A discussion of the validity of such a relationship follows.

Assuming, *a priori* that the Lambert-Beer Law applies to the carbonyl band formed during oxidation in the bulk phases, it can be shown that

$$\frac{(AA)}{d} = K(\lambda)C \quad (1)$$

where (AA) = absorbance area; d = thickness of film; $K(\lambda)$ = constant whose value depends upon the type of functional group being detected by infrared spectroscopy and upon the wavelength limits used in calculating (AA) (see Fig. 2); and C = concentration of functional group being detected. In order to check eq. (1), known amounts of each of the following materials (Aldrich Chemical Co.), undecylenic aldehyde, 6-undecanone, 10-undecenoic acid, and methyl-10-undecenoate, were added to a known amount of APP in carbon tetrachloride. From these solutions were cast films of APP, 2.5 mils thick, weighing 7.5 mg, and infrared spectra of the carbonyl region were taken at ambient temperature. Absorbance areas (AA) were plotted against carbonyl concentration, $[>C=O]$, per 7.5-mg sample (2.5 mils thick). The following relationships were obtained:

$$(AA) = 2.7 \times 10^5 [>C=O]_{AK} \quad (2)$$

where $2.7 \times 10^5 = K(\lambda)d$; and $[>C=O]_{AK}$ = moles of carbonyl of either aldehyde or ketone per 7.5 mg. sample; and

$$(AA) = 6.7 \times 10^5 [>C=O]_{ACE} \quad (3)$$

where $[>C=O]_{ACE}$ = moles of carbonyl of either acid or ester per 7.5 mg film sample. In obtaining eqs. (2) and (3), a small correction was applied for the presence of a very weak carbonyl absorption band in the unoxidized sample of APP.

Relationships (2) and (3) were tested for effects of additivity. Thus, an equimolar mixture of each carbonyl-containing compound was mixed with APP, as described previously. From eqs. (2) and (3), the following expression should hold:

$$(AA) = 4.7 \times 10^5 [>C=O]_T \quad (4)$$

where $[>C=O]_T$ = total number of moles of carbonyl-containing compounds. From the experimental values obtained for the mixture the expression,

$$(AA) = 4.78 \times 10^5 [>C=O]_T \quad (4a)$$

was found to apply. Equations (4) and (4a) are in excellent agreement. From the preceding, we may write (7.5-mg sample)

$$(AA)_T = 2.7 \times 10^5 [>C=O]_{AK} + 6.7 \times 10^5 [>C=O]_{ACE}. \quad (5)$$

Estimation of Various Carbonyl Groups Present

The amounts of the various types of carbonyl-containing compounds were estimated as follows. Standard films of APP were oxidized at 120°C and 20% oxygen, and at 130°C and 100% oxygen from reaction times varying from 40 to 360 min. The corresponding carbonyl absorbance areas were measured. After such measurements, the films were dissolved in a mixture of *n*-butanol and carbon tetrachloride (1:4 by volume). (Both solvents were free of carbonyl groups.) To this solution were

added 1 ml of a saturated solution of 2,4-dinitrophenylhydrazine (DNPH) and one drop of concentrated hydrochloric acid. The flask was loosely stoppered and heated for 30 min at 50°C. After cooling, 5 ml of potassium hydroxide solution was added. The resulting solution was diluted to 25 ml with the mixture of solvents and subjected to colorimetric analysis for aldehydes and/or ketones²⁰ at a wavelength of 480 m μ and a slit width of 0.48, using a Beckman DU spectrophotometer. A blank determination was made simultaneously. The absorbances at 480 m μ were correlated with the carbonyl content for aldehydes and/or ketones from a calibration curve obtained as follows. To known amounts of 6-undecanone in the mixture of solvents previously mentioned were added 1 ml of the solution of DNPH and one drop of concentrated hydrochloric acid. This solution was treated in the same manner as described above, diluted to 25 ml, and subjected to optical analysis at 480 m μ . From such data a calibration curve was obtained for absorbance versus carbonyl concentration (moles carbonyl per 25 ml solution). In this manner could be determined quantitatively the amount of carbonyl in oxidized APP films as aldehyde and/or ketone ($[>C=O]_{AK}$), which was found to be constant under various experimental conditions. Then, from eq. (5), values of $[>C=O]_{ACE}$ could be determined under the same experimental conditions. Thus, the following results were obtained: $[>C=O]_{AK} = (15 \pm 2)$ wt-%; and $[>C=O]_{ACE} = (85 \pm 2)$ wt-% (by difference); and the following expressions obtains (7.5-mg sample):

$$(AA)_T = (6.1 \pm 0.8) \times 10^5 [>C=O]_T \quad (6)$$

It was possible to determine whether the main contribution to the value of $[>C=O]_{ACE}$ was due to acid or ester. After 100 min of oxidation at 130°C and 100% oxygen, the sample of APP was dissolved in carbon tetrachloride, and the infrared spectrum was obtained. This spectrum was compared with those obtained using 10-undecenoic acid and methyl-10-undecenoate. The ester spectrum exhibited a band at 8.55 μ (1170 cm⁻¹) which was absent in the spectrum obtained for the acid. A spectrum of the oxidized sample of APP showed no band at this wavelength, denoting the absence of ester. However, the strong band at 5.83 μ denotes the presence of acid groups.¹⁹ Therefore, it is apparent that the contribution to the value of $[>C=O]_{ACE}$ is due to carboxylic acids alone.

Effect of Sample Thickness

APP films of various thicknesses, 1.1, 2.5, 3.4, and 7.5 mils, were subjected to oxidation at 130°C and 100% oxygen for various reaction times in order to determine whether diffusion control existed for the 2.5-mil thick film used in the oxidation studies. Film thickness was correlated with absorbances at 7.25 μ (1380 cm⁻¹) (absorbance of the CH₃-CH< group in APP) and a linear relationship was observed between absorbance at 7.25 μ and film thickness.

For a particular reaction time, the carbonyl absorbance area was ascertained along with the peak absorbance at 7.25μ . In this manner, values of $(AA)/d$ [cf. eq. (1)] could be determined at various times. When diffusion control does not exist, these values should be constant for various

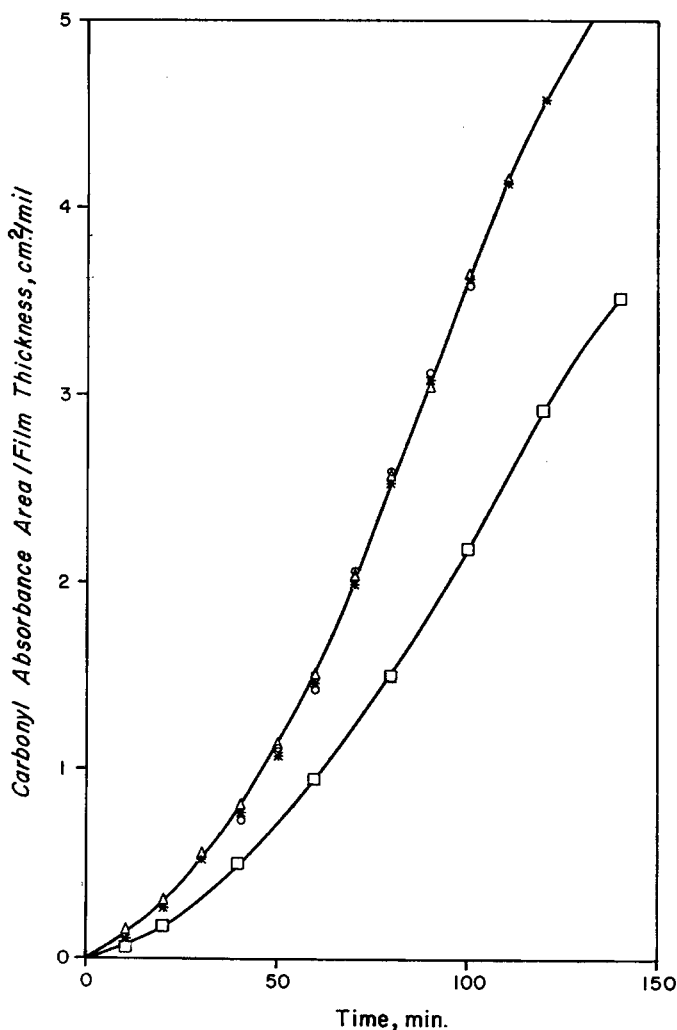


Fig. 3. Effect of APP film thickness on rate of oxidation at 130°C and 100% oxygen: (Δ) 1.1 mil; (\times) 2.5 mil; (\odot) 3.4 mil; (\square) 7.5 mil.

film thicknesses for a particular time. From Figure 3, it can be seen that diffusion control did not appear to exist for film thicknesses of 1.1, 2.5, and 3.4 mils. However, at 7.5 mils thickness, diffusion control apparently began to become important.

RESULTS

As in the cases of IPP,²⁻⁶ APB,⁷ and IPB,⁸ it was observed that for APP, at all oxygen concentrations employed, the reaction rate increased while the induction period decreased with increasing reaction temperature (Fig. 4). Further, as the oxygen concentration was increased, the rate of formation of total carbonyl increased while the induction time decreased, at any one given temperature.

TABLE I
Comparison of Theoretical and Observed Maximum Rates
(ρ_m) of Total Carbonyl at Various Temperatures and
Oxygen Concentrations

Temp, °C	[O ₂], vol-%	K ₁ × 10 ⁴	K ₂	K ₃	ρ_m , cm ² /min	
					Calcd	Obsd
110	5	2.15	26.99	34.88	0.0033	—
	10				0.0054	0.0055
	20				0.0085	0.0090
	50				0.0158	0.0180
	75				0.0214	—
	100				0.0269	0.0265
115	5	3.55	29.60	38.03	0.0057	—
	10				0.0092	0.0090
	20				0.0145	0.0140
	50				0.0267	0.0270
	75				0.0361	0.0370
	100				0.0452	0.0440
120	5	5.50	35.20	44.00	0.0098	0.0100
	10				0.0158	0.0150
	20				0.0244	0.0220
	50				0.0440	0.0450
	75				0.0586	0.0560
	100				0.0728	0.0740
125	5	7.40	39.87	48.65	0.0144	0.0140
	10				0.0231	0.0220
	20				0.0353	0.0380
	50				0.0621	0.0640
	75				0.0819	0.0830
	100				0.1011	0.1000
130	5	9.20	48.62	57.60	0.0206	0.0220
	10				0.0328	0.0310
	20				0.0493	0.0470
	50				0.0839	0.0865
	75				0.1089	0.1120
	100				0.1330	0.1340
135	5	11.60	55.25	64.48	0.0283	0.0315
	10				0.0449	0.0420
	20				0.0670	0.0690
	50				0.1121	0.1120
	75				0.1441	—
	100				0.1747	0.1760

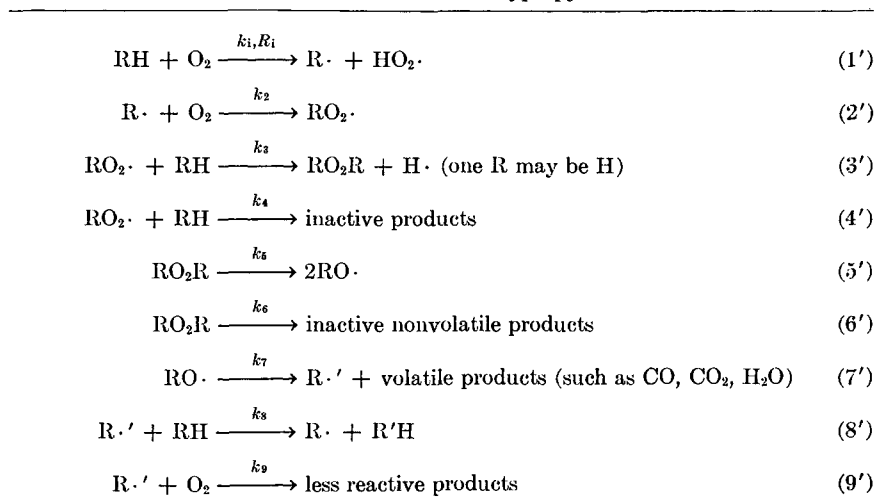
K₁, K₂, K₃ defined in Eqs. (7a), (7b) and (7c)

Maximum rates of formation of total carbonyl (ρ_m) were determined from plots of carbonyl absorbance area versus time (cf. Fig. 4) for various temperatures and oxygen concentrations. These values are listed in Table I. Figure 5 has been constructed from the data in Table I.

DISCUSSION

The reaction scheme and assumptions presented previously² were also used for the APP. For convenience, the scheme is reproduced below in Table II.

TABLE II
Kinetic Scheme for Uncatalyzed Thermal
Oxidation of Isotactic Polypropylene²



The pertinent expressions which were derived are summarized in eqs. 7-10.

$$\rho_m = \frac{K_1[\text{O}_2]}{1 - K_2/(K_3 + [\text{O}_2])} \quad (7)$$

where

$$K_1 = \frac{Ck_2k_3k_6[\text{RH}]}{(k_3 + k_4)(k_5 + k_6)} \quad (7a)$$

and $C = (1 - e^{-At_m}) \approx \text{const.}$, since At_m (where t_m = time to reach maximum reaction rate) is approximately constant under the experimental conditions used (1.2 ± 0.1) over the range of temperatures and oxygen concentrations employed.

$$K_2 = \frac{2k_3k_5k_8[\text{RH}]}{k_9(k_3 + k_4)(k_5 + k_6)} \quad (7b)$$

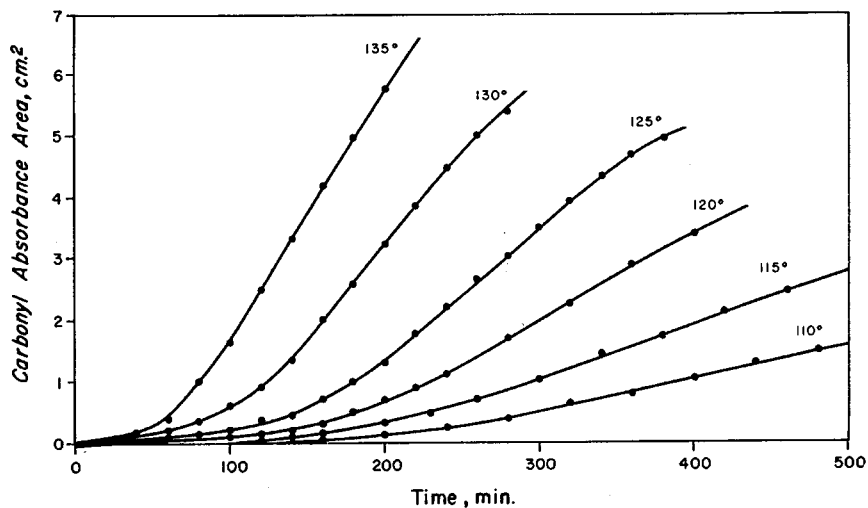


Fig. 4. Plots of carbonyl absorbance area versus time for APP at an oxygen to nitrogen ratio of 10/90 for various temperatures.

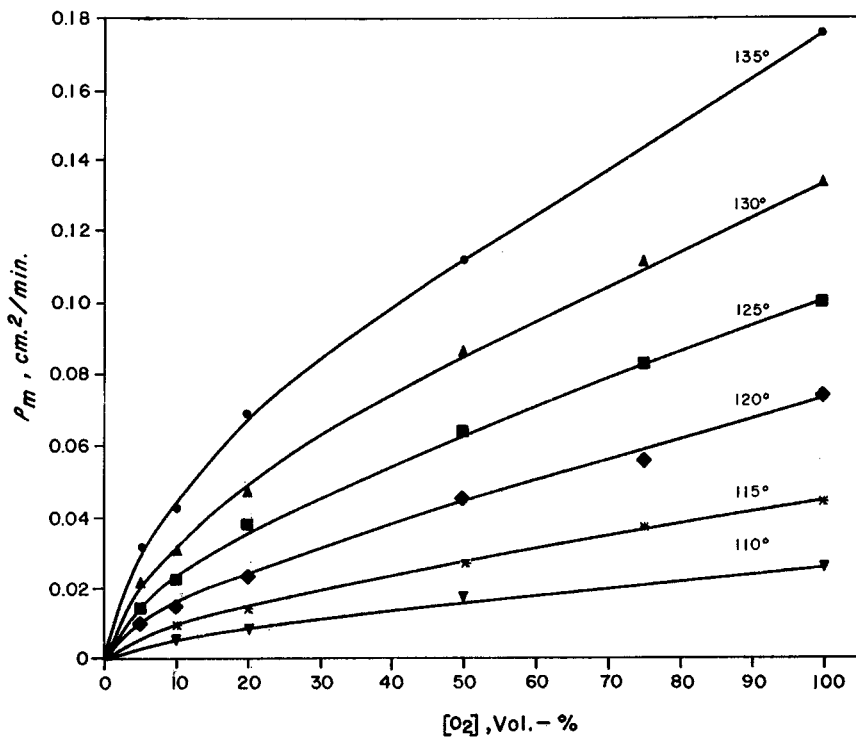


Fig. 5. Plots of maximum rate (ρ_m) versus oxygen concentrations $[O_2]$ at various temperatures for APP.

$$K_3 = \frac{k_8}{k_9}[\text{RH}] \tag{7c}$$

$$k_5 = \frac{(k_3 + k_4)k'K_2}{2k_3K_3} \tag{8}$$

$$A' = 1 - \frac{K_2}{K_3 + [\text{O}_2]} \tag{9}$$

where

$$A' = \frac{A}{k'} = \frac{A}{k_5 + k_6} \tag{9a}$$

and

$$-\ln(\rho_m - \rho)/\rho_m = At \tag{10}$$

when $\rho \ll \rho_m$.

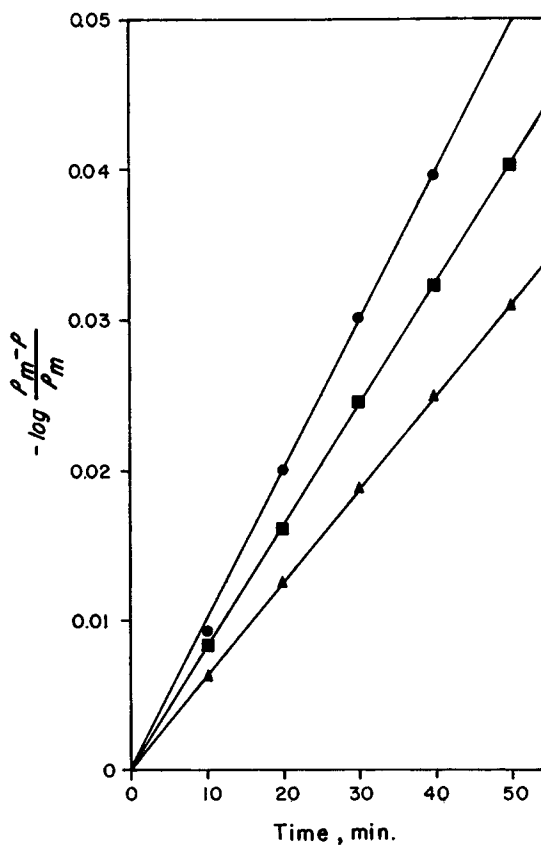


Fig. 6. Plots of $\log [(\rho_m - \rho)/\rho_m]$ versus time at 115°C and various oxygen concentrations: (▲) 20%; (■) 50%; (●) 100%.

For relatively low values of $[O_2]$, eq. (7) becomes

$$\rho_m = \frac{K_1 K_3 [O_2]}{K_3 - K_2} \quad (7d)$$

and for relatively high values of $[O_2]$, eq. (7) becomes

$$\rho_m = K_1 K_3 + K_1 [O_2] \quad (7e)$$

From Figure 5, values of K_1 , K_2 , and K_3 were obtained by means of eqs. (7d) and (7e). Values for these constants are given in Table I for various

TABLE III
Values of A , A' , and k' for Various
Temperatures and Oxygen Concentrations

Temp, °C	$[O_2]$, vol-%	A'	$A \times 10^3$, min ⁻¹	$k' \times 10^3$, min ⁻¹	$k' \times 10^3$ (av.), min ⁻¹
110	5	0.3232	—	—	1.915
	10	0.3986	0.970	1.908	
	20	0.5082	—	—	
	50	0.6820	1.212	1.777	
	75	0.7544	—	—	
	100	0.7999	1.647	2.059	
115	5	0.3121	—	—	2.874
	10	0.3838	—	—	
	20	0.4899	1.446	2.952	
	50	0.6638	1.874	2.873	
	75	0.7381	2.065	2.798	
	100	0.7856	2.300	2.923	
120	5	0.2816	—	—	4.351
	10	0.3482	—	—	
	20	0.4500	2.104	4.667	
	50	0.6255	2.572	4.112	
	75	0.7042	3.103	4.407	
	100	0.7556	3.180	4.208	
125	5	0.2569	—	—	6.297
	10	0.3202	—	—	
	20	0.4192	2.579	6.009	
	50	0.5959	3.739	6.274	
	75	0.6776	4.312	6.364	
	100	0.7318	4.786	6.540	
130	5	0.2233	—	—	10.791
	10	0.2808	—	—	
	20	0.3735	4.238	11.347	
	50	0.5482	5.757	10.516	
	75	0.6333	6.684	10.554	
	100	0.6915	7.433	10.749	
135	5	0.2048	—	—	18.183
	10	0.2582	—	—	
	20	0.3460	6.190	17.890	
	50	0.5178	9.540	18.438	
	75	0.6039	—	—	
	100	0.6641	12.100	18.220	

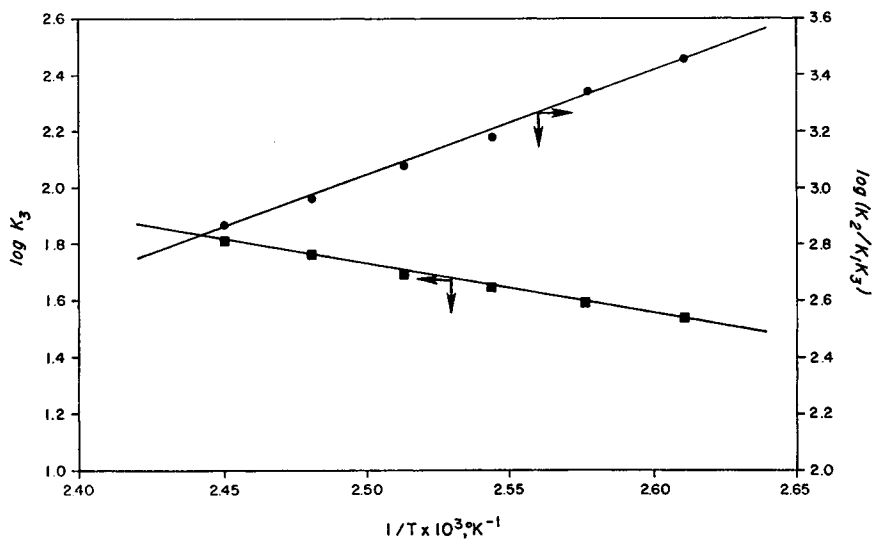


Fig. 7. Plots of $\log K_3$ and $\log (K_2/K_1K_3)$ versus reciprocal temperature, $1/T$.

temperatures and oxygen concentrations. From these values, various values of ρ_m were calculated and found to agree well with observed values (cf. Table I). Estimates of K_2 were obtained using eq. (7d), and by arbitrarily drawing initial slopes in Figure 5 such that the values obtained would best agree with experimental points. From eq. (10), values of A were determined at various temperatures and oxygen concentrations (Fig. 6) and are given in Table III. Corresponding values of A' were calculated from eq. (9), and then values of k' were determined from eq. (9a). The values of k' , at a given temperature and for various oxygen concentrations, were about constant, as anticipated (cf. Table III).

Arrhenius plots of $\log K_3$ and $\log [K_2/(K_1K_3)]$ were constructed as shown in Figure 7. From the slopes of the linear relationships obtained and from eqs. (7a) to (7c), the following values were obtained: $E_8 - E_9 \approx 8$ kcal/mole, and $E_i + E_8 - E_5 \approx 17$ kcal/mole. From eq. (8), it can also be seen that if k_4/k_3 is constant over the temperature range used (this was previously indicated to be approximately true²¹), then an Arrhenius plot of $\log [(k'K_2)/K_3]$ should afford a value of E_5 . In this manner, $E_5 \approx 31$ kcal/mole (cf. Fig. 8). This value was checked by means of a plot of $\log (\rho_m A/[O_2])$ versus reciprocal temperature [cf. Fig. 8 and eqs. (7), (7a), and (9a)] to yield a value of $E_i + E_6 \approx 48$ kcal/mole from which a value of $E_5 \approx 31$ kcal/mole was calculated. The value obtained for E_5 agrees well with that generally found for the unimolecular decomposition of hydroperoxides (30 kcal/mole).²²

Values of the various parameters obtained in this work for APP are compared with corresponding values reported for IPP² in Table IV. From this table, it can be seen that various values of activation energies and

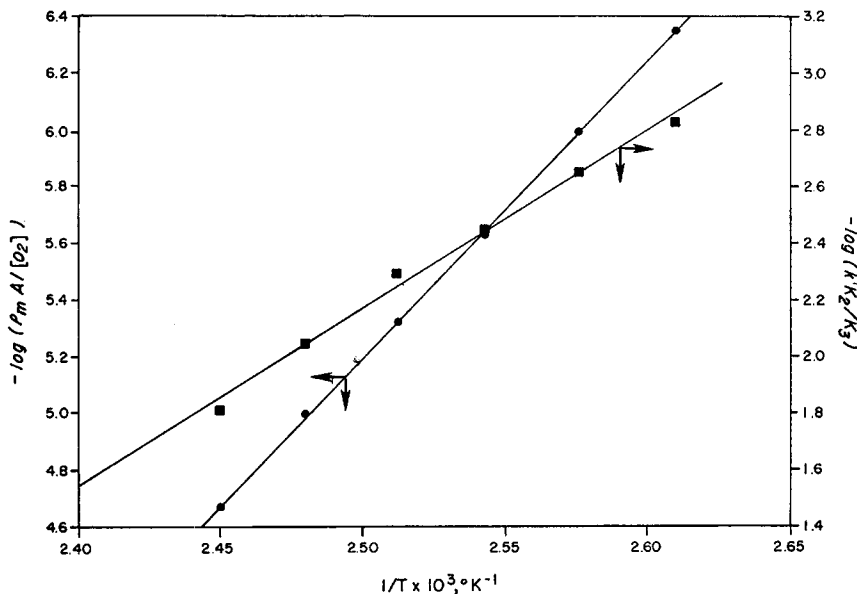


Fig. 8. Plots of $\log (\rho_m A / [O_2])$ and $\log (k' K_2 / K_3)$ versus reciprocal temperature, $1/T$.

TABLE IV
Comparison of Various Parameters Obtained
During APP Oxidation with Those Reported for IPP Oxidation

Kinetic parameters	APP	IPP ^a
k' , min^{-1} (140°C)	0.03 (extrapolated)	0.047
E_5 , kcal/mole	31	33
$E_i + E_6 - E_5$, kcal/mole	17	18
$E_i + E_6$, kcal/mole	48	51
$E_8 - E_9$, kcal/mole	9	6
(ash, %)	(0.008)	(0.02)

^a From Stivala et al.²

rate constants are similar. A possible explanation follows. It is assumed that the IPP is comprised of a fringed micellar structure wherein the crystallite regions are essentially separated from the amorphous regions. The former regions presumably do not act as a continuous barrier to oxygen penetration. Thus, diffusion control is not important at small film thicknesses both for APP and IPP. Furthermore, the isolated amorphous regions in IPP react similarly to those in APP in respect to oxidizability. Consequently, similar rate constants would be anticipated for APP and IPP. In this connection, Hawkins and co-workers²³ observed a relatively small difference in the rates of oxidation between APP and IPP. Wiles and co-workers²⁴ also found that the rate of photochemical oxidation of polypropylene of various tacticities did not change appreciably. Thus, IPP samples oxidized somewhat faster as compared with those of APP.

This work was supported in part by a grant from the Office of Naval Research to the Stevens Institute of Technology.

References

1. L. Reich and S. S. Stivala, *Autoxidation of Hydrocarbons and Polyolefins*, M. Dekker, Inc., New York, 1969.
2. S. S. Stivala, L. Reich, and P. G. Kelleher, *Makromol. Chem.*, **59**, 28 (1963).
3. L. Reich and S. S. Stivala, *J. Polym. Sci. B*, **3**, 227 (1965).
4. S. S. Stivala and L. Reich, *Polym. Eng. Sci.*, **5**, 179 (1965).
5. L. Reich and S. S. Stivala, *J. Polym. Sci. A*, **3**, 4299 (1965).
6. L. Reich and S. S. Stivala, *Rev. Macromol. Chem.*, **1**, 249 (1966).
7. S. S. Stivala, E. B. Kaplan, and L. Reich, *J. Appl. Polym. Sci.*, **9**, 3557 (1965).
8. S. S. Stivala, G. Yo, and L. Reich, *J. Appl. Polym. Sci.*, **13**, 1289 (1969).
9. M. B. Neiman, *Russ. Chem. Rev.*, **33**, 11 (1964).
10. V. B. Miller, M. B. Neiman, V. S. Pudov, and L. I. Lafer, *Vysokomol. Soedin.*, **1**, 1696 (1959).
11. M. P. Schard and C. A. Russell, *J. Appl. Polym. Sci.*, **8**, 895 (1964).
12. G. E. Ashby, *J. Polym. Sci.*, **50**, 99 (1961).
13. L. Reich and S. S. Stivala, *J. Appl. Polym. Sci.*, **12**, 2033 (1969).
14. E. Beati, F. Severini, and G. Clerici, *Makromol. Chem.*, **61**, 104 (1963).
15. C. E. H. Bawn and S. A. Chaudhri, *Polymer*, **9**, 81 (1968).
16. C. E. H. Bawn and S. A. Chaudhri, *Polymer*, **9**, 123 (1968).
17. C. E. H. Bawn and S. A. Chaudhri, *Polymer*, **9**, 113 (1968).
18. L. Reich and S. S. Stivala, *J. Appl. Polym. Sci.*, **13**, 23 (1969).
19. J. P. Luongo, *J. Appl. Polymer Sci.*, **3**, 302 (1960).
20. G. R. Lappin and L. C. Clark, *Anal. Chem.*, **23**, 541 (1951).
21. L. Reich and S. S. Stivala, *J. Appl. Polym. Sci.*, **13**, 17 (1969).
22. N. Uri, in *Autoxidation and Antioxidants*, W. O. Lundberg, Ed., Wiley-Interscience, New York, 1961, Vol. 1, p. 90.
23. W. L. Hawkins, W. Matreyek, and F. H. Winslow, *J. Polym. Sci.*, **41**, 1 (1959).
24. Y. Kato, D. J. Carlsson, and D. M. Wiles, *J. Appl. Polym. Sci.*, **13**, 1447 (1969).

Received April 21, 1970